

The Mining Area Land Surface Temperature Retrieval from Landsat-8 Data

Chunsen Zhang* and Rongrong Wu
Xi'an University of Science and Technology, China.
Email: zhchunsen@aliyun.com

Keywords: Surface temperature retrieval, Landsat-8, mining area, Mono-window algorithm

Abstract: Taking the Shendong mining area as a research area, Landsat-8 data were used to retrieve the surface temperature of the study area using the radiation conduction equation method, the image-based retrieval algorithm (IB algorithm), the Mono-window algorithm (MW algorithm) and the single-channel algorithm (SC algorithm) respectively. The data were validated by MODIS land surface temperature (LST) data, comparing the similarities and differences between different algorithms. The results show that: (1) The Mono-window algorithm inversion accuracy is the highest among the four surface temperature inversion algorithms, which is the closest to MODIS LST data, followed by the radiation conduction equation, SC algorithm and IB algorithm. (2) The retrieval results of bare soil and buildings are the best for the four kinds of landform types, of which MW algorithm has the highest retrieval accuracy. (3) The MW algorithm should be adopted for the retrieval of surface temperature based on Landsat-8 data in the mining area.

1 INTRODUCTION

The exploitation and utilization of mineral resources provide the backbone for the economic construction and social development of the society, and inevitably cause great damage to the ecological environment in the mining area (QIU and HOU, 2013). However, as an important hydrological, meteorological and environmental parameter, surface temperature affects the exchange of sensible and latent heat between Earth-gas and it has important applications in many fields, especially in the meteorology, hydrology, vegetation ecology and environmental monitoring (Li et al., 2016). Surface temperature is an important parameter in the physical processes of the Earth's surface at the regional and global scales and it also plays an important role in the Earth-gas interaction (Hu et al., 2015). Using satellite observations, thermal infrared remote sensing images can quickly and easily obtain large surface temperature data. The data are updated quickly and the cost is low. Therefore, thermal infrared remote sensing data is widely used in surface temperature retrieval (Zheng and Zeng, 2011). Landsat satellite data has always been one of the most important remote sensing data for retrieval

of surface temperature. In 2013, NASA successfully launched the Landsat 8 satellite which has two thermal infrared bands, the 10th and 11th bands. The Landsat 8 data has more advantages than previous Landsat series satellites on surface temperature retrieval.

At present, the main methods of surface temperature retrieval are the radiation conduction equation method, the image-based retrieval algorithm, the Mono-window algorithm proposed by Qin et al. (2001) and the Single-channel algorithm proposed by Jiménez-Muñoz et al (2003). As early as 2004, Sobrino et al (2004) used Landsat 5 TM thermal infrared data to compare the similarities and differences among the radiation conduction equation method, the Mono-window algorithm and the Single-channel algorithm. In 2009, Fan Hui (2009) also introduced the Landsat data retrieval algorithm. In 2016, Windahl et al. (2016) also performed surface retrieval using the radiation conduction equation, Mono-window algorithm and Single-channel algorithm. According to the different remote sensing data and the actual situation of different research areas, scholars at home and abroad have proposed a variety of surface temperature retrieval algorithms, as well as comparatively analyze several

surface temperature retrieval algorithms. However, there are few studies on land surface temperature retrieval of Landsat 8 data. In this paper, based on the Landsat 8 data, using the Shendong mining area as the study area, the results of the four surface temperature retrieval algorithms are compared to obtain the surface temperature retrieval algorithm which is the most suitable for the mining area, so as to facilitate the study of ecological environment in mining area. It has great significance for environmental assessment and ecological reconstruction of mining areas.

2 DATA AND WORKFLOW

2.1 Study Area Summary

Shendong mining area is located in the junction of Shaanxi and Inner Mongolia provinces. It was built in 1985, and located in the transition zone between the Mu Us Desert and Shaanxi Loess Plateau. Its geographic range is (Latitude 38°52'-39°41' north, Longitude 109°51'-110°46' east) and its central geographic coordinates are (39°11'30" N, 110°18'30" E). And its average elevation is 1.2km, showing a general trend of low south and low north (Figure 1). Annual precipitation is less and belongs to the semiarid continental climate. Shendong mining area belongs to a typical arid or semi-arid desert area in northwestern China with low vegetation coverage. In recent years, due to the intensification of mining activities, the ecological environment in the area has further deteriorated.

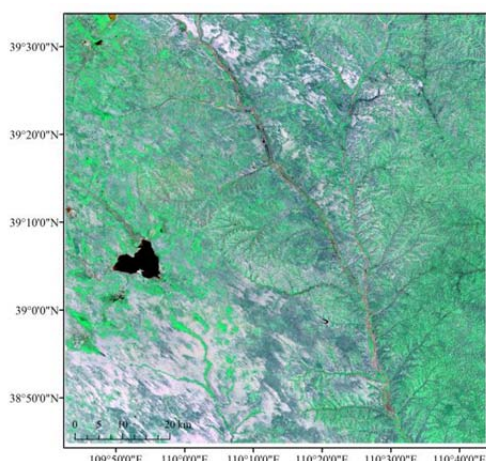


Figure 1: Location map of Shendong mining area.

2.2 Data Introduction

On February 11, 2013, NASA successfully launched the Landsat 8 satellite, reintroducing fresh blood into the Landsat program that has taken 40 years. The Landsat-8 carries two main payloads: the OLI (Operational Land Imager) and the TIRS (Thermal Infrared Sensor). The OLI Terrestrial Imager includes nine bands with a spatial resolution of 30 meters, including a 15-meter panchromatic band with an imaging wide band of 185x185km. The OLI includes all the bands of the ETM+ sensor and two additional bands: blue band (band 1; 0.433-0.453 μm) Main applications in Coastal band observations, shortwave IR band (band 9; 1.360-1.390 μm) Includes Strong water vapor absorption characteristics can be used for cloud detection; Near-infrared band 5 and short-wave infrared band 9 are closer to the band corresponding to MODIS.

Based on the Landsat-8 data of Shendong mining area from October 5, 2015, four surface temperature retrieval algorithms are used: the radiation conduction equation method, image-based algorithm, Mono-window algorithm and Single-channel algorithm to retrieve the surface temperature of the study area. And land surface temperature (1km, daily) product data of the same day were respectively used for verification. Data preprocessing includes: Radiation correction of the original image, atmospheric correction, eliminating the impact of the atmosphere on the image, image cropping, cutting out the Shendong mining area. Work flow chart is as follows (Figure 2):

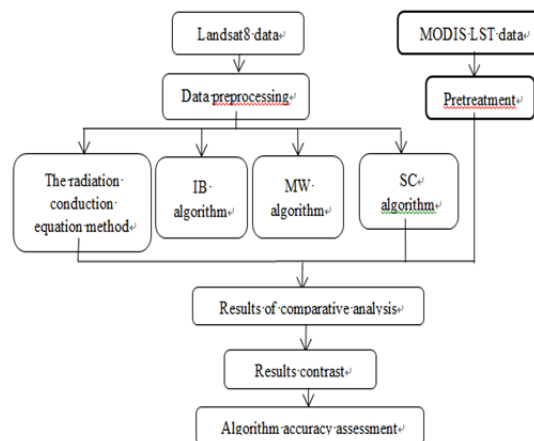


Figure 2: Workflow diagram.

3 SURFACE TEMPERATURE RETRIEVAL

3.1 Surface Emissivity Calculation

Calculation of surface emissivity, using NDVI threshold method to calculate surface emissivity (Li et al., 2016):

$$\varepsilon = 0.004P_v + 0.986 \quad (1)$$

Among them, p_v is the vegetation coverage, which is calculated by the pixel dichotomy. The principle is as follows (Li et al., 2016):

$$p_v = \frac{(NDVI - NDVI_{soil})}{(NDVI_{veg} - NDVI_{soil})} \quad (2)$$

In the formula, $NDVI_{soil}$ is the $NDVI$ value of the bare soil cover area; $NDVI_{veg}$ is the $NDVI$ value of the complete vegetation cover area; $NDVI$ is the normalized vegetation index, calculated according to the following formula:

$$NDVI = \frac{(b_4 - b_3)}{(b_4 + b_3)} \quad (3)$$

In the above formula, b_4 is the near-infrared band and b_3 is the red band, and the normalized vegetation index is calculated according to the two bands.

Statistically calculated $NDVI$ value, $NDVI_{soil}$ is taken as the $NDVI$ accumulated 5% and $NDVI_{veg}$ is taken as 95% of the pixel value.

3.2 The Radiation Conduction Equation Algorithm

The expression of surface temperature retrieval according to the radiation conduction equation is (Wu et al., 2016):

$$T_s = \frac{K_2}{\ln\left(\frac{K_1}{B(T_s)} + 1\right)} \quad (4)$$

In the above formula, K_1 and K_2 are the calibration constants for the sensor.

$$K_1 = 774.89 \left(\frac{w}{m^2} \cdot sr \cdot \mu m \right),$$

$$K_2 = 1321.08(K),$$

$B(T_s)$ is blackbody radiance of temperature calculated as follows:

$$B(T_s) = \frac{[L_\lambda - L^\uparrow - \tau \times (1 - \varepsilon) \times L^\downarrow]}{(\tau \times \varepsilon)} \quad (5)$$

In the above formula, τ is atmospheric transmittance, L^\uparrow is atmospheric up radiation, and L^\downarrow is atmospheric down radiation. The three parameters can be found by entering the relevant parameters through the NASA website (<https://atmcorr.gsfc.nasa.gov/>); L_λ is the radiation brightness of the thermal infrared spectrum received by the sensor. ε is the surface emissivity.

3.3 Image-Based Retrieval Algorithm

The Image-based Method (IB algorithm) is to invert the DN value of the thermal infrared band to ground bright temperature.

The IB algorithm calculates the surface temperature as follows (Ding and Xu, 2008):

$$T_s = \frac{T_{red}}{1 + \left(\lambda \cdot \frac{T_{red}}{\rho} \right) \ln \varepsilon} \quad (6)$$

In the above formula, T_s is surface temperature; λ is thermal infrared center wavelength; T_{red} is surface bright temperature which can be converted to the surface bright temperature through the radiation correction of the DN value of the thermal infrared band.

$\rho = h \times c / \sigma (1.438 \times 10^{-2} mk)$, ε is surface emissivity.

3.4 Mono-Window Algorithm

Mono-window algorithm (MW algorithm) was proposed by Qin Zhihao et al in 2001. The retrieval surface temperature algorithm is calculated as:

$$T_s = \frac{[a \times (1 - C - D) + (b \times (1 - C - D) + C + D) \times T_e - D \times T_a]}{C} \quad (7)$$

$$C = \varepsilon \times \tau \quad (8)$$

$$D = (1 - \tau) \times [1 + (1 - \varepsilon) \times \tau] \tag{9}$$

In the above formula, ε is surface emissivity; T_6 is surface bright temperature; a and b are constants, respectively -67.355351 and 0.458606; T_a is the average temperature of the atmosphere. τ is atmospheric transmittance. According to the location of the study area, temperature and water vapor, the calculation method can be calculated according to the following formula (Li et al., 2016):

$$T_a = 16.0110 + 0.92621(t + 273.15) \tag{10}$$

$$\tau = 0.974290 - 0.08007\omega \tag{11}$$

ω is atmospheric moisture content, the calculation formula is as follows (Li et al., 2016) :

$$\omega = 0.0981 \times \left(6.1078 \times 10^{\left(\frac{7.5t}{t+273.3} \right)} \right) \times RH + 0.1697 \tag{12}$$

t is the average temperature of the atmosphere, RH is the relative humidity. They can be obtained through the China weather station network data.

3.5 Single-Channel Algorithm

The Single-Channel Method (SC-Algorithm) was proposed by Jiménez-Muñoz (Jiménez and Sobrino, 2003) in 2003 and is calculated as follows:

$$T_s = \gamma [\varepsilon^{-1} (\psi_1 L_{sen} + \psi_2) + \psi_3] + \delta \tag{13}$$

In the formula, ε is the surface emissivity; L_{sen} is the radiation intensity measured by remote sensor for satellite height;

$\gamma, \delta, \psi_1, \psi_2, \psi_3$ are intermediate variables, the formula is as follows (Xu et al., 2015):

$$\gamma = \frac{T_{sen}^2}{(b_\gamma L_{sen})} \tag{14}$$

$$\delta = T_{sen} - \frac{T_{sen}^2}{b_\gamma} \tag{15}$$

$$b_\gamma = C_2 \left(\frac{\lambda^4}{C_1} + \frac{1}{\lambda} \right) \tag{16}$$

Among them, T_{sen} is the ground brightness temperature, λ is the thermal infrared band center wavelength; C_1 and C_2 are constants:

$$C_1 = 1.19104 \times 10^8 (w \cdot \mu m^4 \cdot m^{-2} \cdot sr^{-1}),$$

$$C_2 = 14387.7 (\mu m \cdot k),$$

$$\psi_1 = a_{11}\omega^2 + a_{12}\omega + a_{13} \tag{17}$$

$$\psi_2 = a_{21}\omega^2 + a_{22}\omega + a_{23} \tag{18}$$

$$\psi_3 = a_{31}\omega^2 + a_{32}\omega + a_{33} \tag{19}$$

The parameters are shown in the following table 1 (Ding and Xu, 2006):

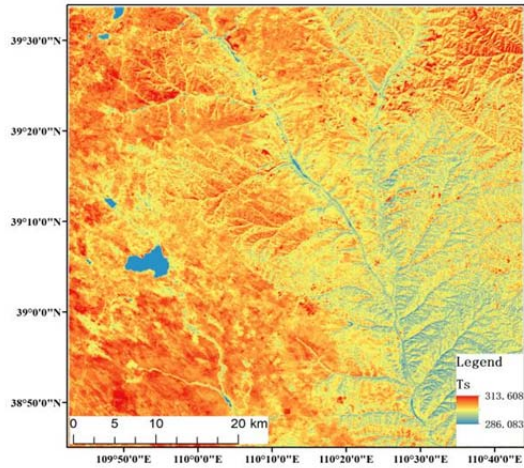
Table 1: Parameter values.

Parameter	Landsat TM/ETM+	Landsat OLI
a_{11}	0.14714	0.04019
a_{12}	-0.15583	0.02916
a_{13}	1.1234	1.01523
a_{21}	-1.1836	-0.38333
a_{22}	-0.37607	-1.50294
a_{23}	-0.52894	0.20324
a_{31}	-0.04554	0.00918
a_{32}	1.18719	1.36072
a_{33}	-0.39071	-0.27514

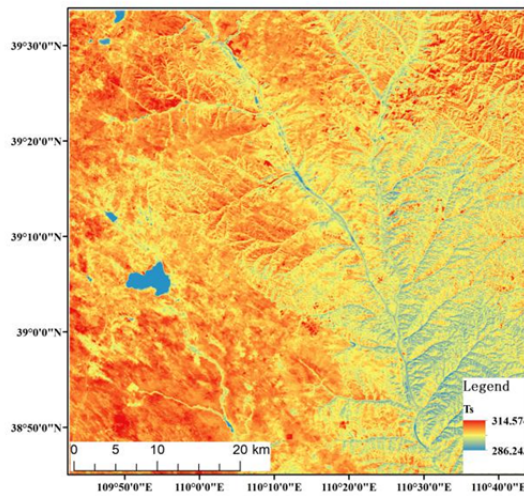
4 SURFACE TEMPERATURE RETRIEVAL RESULTS AND ACCURACY ASSESSMENT

The retrieval results of the four surface temperature retrieval algorithms are not much different, among them the MW algorithm and the radiation conduction equation method are the closest, the surface temperature values of the study area retrieved by the two algorithms are relatively high. The result of SC algorithm is higher than the surface temperature retrieved by the MW algorithm and the radiation conduction equation algorithm (Figure 3). The high-temperature areas are mainly distributed in

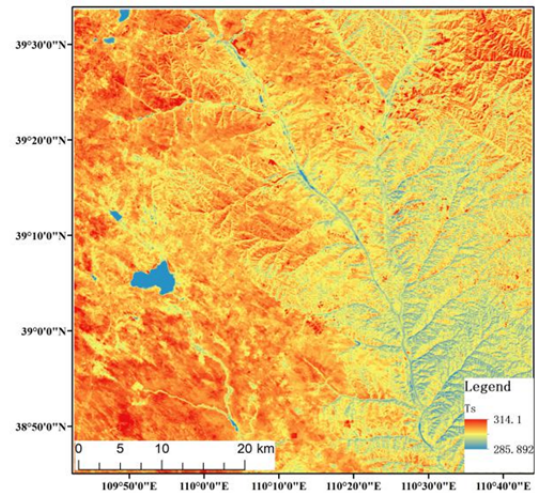
the north and west of Shendong mining area, the middle-temperature areas are concentrated in the central area, and the eastern areas with high vegetation coverage are basically low-temperature areas.



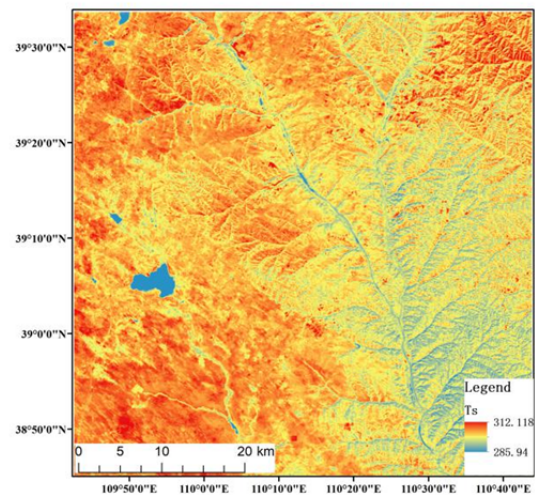
(a) MW algorithm



(b) SC algorithm



(c) The radiation conduction equation algorithm



(d) IB algorithm

Figure 3: Surface temperature distribution.

The results of four kinds of temperature retrieval algorithm compared with MODIS LST after data processing. The MODIS LST data needs to be preprocessed first, and then the result of the surface temperature retrieval algorithm is resample to 1 km. The maximum, minimum, and average values of each algorithm and MODIS LST data are calculated.

From the statistical results in Table 2, the maximum, minimum and average of MW algorithm are closest to MODIS LST temperature product data. The four surface temperature retrieval algorithms,

the surface temperature values of MW algorithm and the radiation conduction equation algorithm are relatively close. On average, the difference between the Mono-window algorithm and LST data is about 0.03K; SC algorithm and LST data difference is about 0.58K; Radiation conduction equation method and LST data difference is about 0.19K; IB algorithm is about 0.65K.

Based on four typical types of ground objects, multiple sample points were selected to calculate the average surface temperature. Combine four typical ground objects, select multiple sample points, and calculate the average of their surface temperatures. On the whole, in October 2015, the temperature of the water bodies in the four kinds of feature categories was the lowest, the average is 5K lower than other categories. The surface temperature of bare soil was the highest relative to other features with an average about 298K. The difference in surface temperature between vegetation and buildings was not large, the value is about 297K. The four types of land surface temperature from high to low: bare soil, buildings, vegetation, water.

Comparing and analyzing the results of four surface temperature retrieval algorithms (Table 3), the result of retrieval between water body and MODIS LST data is about 3K, the surface temperature retrieval result of bare soil is about 0.3K, and the result of surface temperature retrieval is 0.5K, and the retrieval result of buildings is about 0.1K, of which the temperature of the water body is the lowest and the temperature of the building is the highest.

5 CONCLUSIONS

Based on Landsat 8 remote sensing images, using Shendong mining area as the research area, the surface temperature of the study area in 2015 is retrieved by four methods of radiation conduction equation, IB algorithm, MW and SC algorithm, and

the result is verified using MODIS LST data respectively. As the result, the differences in the four surface temperature retrieval algorithms were analyzed and compared, and the surface temperature of the mining area was studied. The following conclusions were drawn:

1) According to the results of surface temperature retrieval, the high temperature in Shendong mining area is mainly distributed in the north and the west, the middle temperature is concentrated in the middle part, while the eastern part with high vegetation coverage is basically in the low temperature area, indicating that vegetation cover degree and surface temperature were negatively correlated.

2) Based on Landsat 8 data, the retrieval result of the Mono-window algorithm in the four surface temperature retrieval algorithms is closest to the MODIS LST data. The retrieval result of the Mono-window algorithm has little difference with the radiation conduction method. And the gap between the IB algorithm and MODIS LST data is the largest.

3) The results of surface temperature retrieval algorithms of water bodies in four typical landform types are lower than MODIS LST data. For vegetation, only the SC algorithm has a slightly higher surface temperature retrieval result than the MODIS LST data. The accuracy of IB algorithm is lower than any other ground objects. The retrieval results of the MW algorithm and the radiation conduction equation are similar. The MW algorithm retrieval result is the closest to the MODIS LST data with the highest accuracy. The surface temperature of the four kinds of landform types from high to low: bare soil, buildings, vegetation and water.

4) Based on the Landsat 8 data, the Mono-window algorithm has the highest retrieval accuracy in the four surface temperature retrieval algorithms. Therefore, the Mono-window algorithm can be used for practical application in the study of the ecological environment or other issues in the mining area.

Table 2: Comparison of the four algorithms of Landsat and the data temperature of MODIS product.

Algorithm	Minimum(K)	Maximum(K)	Average(K)
MW	287.334381	309.588928	297.157173
SC	287.534119	310.457642	297.703065
Radiation conduction equation	287.178650	310.004150	297.309012
IB	287.131042	308.295410	296.465504
MODIS LST	290.339996	301.859985	297.120451

Table 3: Comparison of surface temperature retrieval results with MODIS LST data.

Algorithm	Water(K)	Vegetation(K)	Bare soil(K)	Buildings(K)
MW	291.5670145	296.6649273	298.9086183	297.4721965
SC	291.914622	297.2018169	299.5086142	298.0196146
Radiation conduction equation	291.5427124	296.810197	299.1072449	297.6238139
IB	291.1542784	295.9958007	298.131014	296.7675171
MODIS LST	294.502657	297.1853273	298.6946613	297.3679931

REFERENCES

- Ding Feng, Xu Hanqiu 2006 An Algorithm and Experimental Analysis of Surface Temperature Retrieval Based on TM Thermal Wave Image [J] *Journal of Earth Sciences* **8** (3) 125-130
- Ding Feng, Xu Hanqiu 2008 A Comparative Study of Three Land Surface Temperature Retrieval Algorithms Based on Landsat TM *Journal of Fujian Normal University* (Natural Science Edition) **24**(1) 91-96
- Fan Hui 2009 Comparative Analysis of Land Surface Temperature Retrieved from Landsat TM Thermal Infrared Bands [J] *Remote-Sensing Information* **1** 36-40
- Hu DY, Qiao K, Wang XL, et al 2015 A mono-window algorithm combined with Landsat 8 thermal infrared data retrieval of surface temperature *Journal of Remote Sensing* **19**(6) 964-976
- Jiménez-Muñoz J C, Sobrino J A 2003 A generalized single-channel method for retrieving land surface temperature from remote sensing data [J] *Journal of Geophysical Research Atmospheres* **108**(D22) 2015-2023
- Li Hengkai, Yang Liu, Lei Jun, et al 2016 Analysis of surface disturbances in rare earth mining area based on temperature difference *Chinese Journal of Rare Earths* **3** 373-384
- Li Z L, Duan S B, Tang B H, et al. 2016 Research progress on retrieval method of surface temperature by thermal infrared remote sensing *Journal of Remote Sensing* 20(5) 899-920
- Qin Z, Karnieli A, Berliner P 2001 A mono-window algorithm for retrieving land surface temperature from Landsat TM data and its application to the Israel-Egypt border region[J] *International Journal of Remote Sensing* **22**(18) 3719-3746
- QIU Wen-wei, HOU Hu-ping 2013 Study on Surface Temperature Variation of Ecological Disturbance in Mining Area Based on RS [J] *Mining Research and Development* **2** 68-71
- Sobrino J A, Jiménez-Muñoz J C, Paolini L 2004 Land surface temperature retrieval from Landsat TM 5[J] *Remote Sensing of Environment* **90**(4) 434-440
- Windahl E, de Beurs K 2016 An intercomparison of Landsat land surface temperature retrieval methods under variable atmospheric conditions using in situ skin temperature [J] *International Journal of Applied Earth Observation and Geoinformation* **51** 11-27
- Wu Z G, Jiang T, Fan Y L, et al. 2016 Study on surface temperature retrieval and analysis based on Landsat 8 data-A case study in Wuhan *Journal of Engineering Geophysics* **13**(1) 135-142
- Xu Hanqiu, Lin Zhongli, Pan Weihua 2015 study on several problems for retrieval of surface temperature by single channel algorithm - a case study of landsat series data [J] *Journal of Wuhan University* **40**(4) 487-492
- Zheng Wen-wu, Zeng Yong-nian 2011 Comparative Analysis of Multi-source Remote Sensing Data Retrieval Algorithms for Surface Temperature *Journal of Earth Sciences* **13**(6) 840-847